

# Sequence-Specific Binding of DNA to Liposomes Containing Di-Alkyl Peptide Nucleic Acid (PNA) Amphiphiles

Bruno F. Marques and James W. Schneider\*

Department of Chemical Engineering, Carnegie Mellon University,  
Pittsburgh, Pennsylvania 15213-3890

Received August 13, 2004. In Final Form: November 24, 2004

We present a method to covalently attach peptide nucleic acid (PNA) to liposomes by conjugation of PNA peptide to charged amino acids and synthetic di-alkyl lipids ("PNA amphiphile," PNAA) followed by co-extrusion with disterylphosphatidylcholine (DSPC) and cholesterol. Attachment of four Glu residues and two ethylene oxide spacers to the PNAA was required to confer proper hydration for extrusion and presentation for DNA hybridization. The extent of DNA oligomer binding to 10-mer PNAA liposomes was assessed using capillary zone electrophoresis. Nearly all PNAs on the liposome surface are complexed with a stoichiometric amount of complementary DNA 10-mers after 3-h incubation in pH 8.0 Tris buffer. No binding to PNAA liposomes was observed using DNA 10-mers with a single mismatch. Longer DNA showed a greatly attenuated binding efficiency, likely because of electrostatic repulsion between the PNAA liposome double layer and the DNA backbone. Langmuir isotherms of PNAA: DSPC: chol monolayers indicate miscibility of these components at the compositions used for liposome preparation. PNAA liposomes preserve the high sequence-selectivity of PNAs and emerge as a useful sequence tag for highly sensitive bioanalytical devices.

## Introduction

While the use of liposomes as model membranes and in drug and gene delivery applications is well appreciated, their encapsulation properties can also be applied to the creation of highly sensitive bioanalytical devices. A 1000-fold signal amplification can be achieved using liposomes filled with fluorescent material as probes.<sup>1,2</sup> Signal amplification can also be carried out with nonfluorescent liposomes by dendritic amplification, where networks of specifically linked liposomes are bound to surfaces. These networks can be detected by Faradaic impedance spectroscopy or by microgravimetry, with detection limits as low as  $10^{-13}$  M.<sup>3,4</sup> Other biosensing applications rely on the release of electrochemical indicators from the core of liposomes<sup>5–7</sup> or colorimetric transitions of polydiacetylene amphiphiles in the bilayer.<sup>8</sup> Most recently, liposomes have been implemented in microfluidic chips for biosensing purposes.<sup>9, 10</sup>

The unique binding properties of peptide nucleic acids (PNA) give them important advantages in biosensing applications. These synthetic nucleic acid analogues bind complementary DNA to form a PNA–DNA duplex that is

more stable than the corresponding DNA–DNA duplex.<sup>11</sup> PNA is a structural mimic of DNA that replaces the negatively charged sugar–phosphate backbone of DNA with an uncharged *N*-(2-aminoethyl)glycine backbone, and the added stability of PNA–DNA duplexes has been ascribed to the lower degree of charge repulsion for PNA–DNA duplex formation.<sup>12,13</sup> PNA–DNA duplex stabilities are highly sensitive to single-base mismatches.<sup>14</sup> PNA can also bind specific dsDNA targets by triplex formation, even in biological buffers that suppress triplex formation between ssDNA and dsDNA.<sup>15,16</sup> By constructing liposomes hosting PNA in an active form, we should be able to achieve the highly sensitive detection levels afforded by liposomes while adding the highly selective binding properties of PNA.

A difficulty encountered when working with PNAs is that they are sparingly soluble in water and have a tendency to self-aggregate in solution. While these effects have not been studied extensively, PNA oligomers are soluble in water at concentrations below about 10  $\mu$ M, and their solubility is improved by the addition of a terminal lysine group.<sup>17</sup> To better understand their cellular uptake, Wittung et al. measured low rates of efflux of PNA oligomers from the interior of liposomes, indicating that their solubility in the nonpolar lipid bilayer is also fairly low.<sup>18</sup> Hence, the low solubility of PNA in both polar

\* To whom correspondence should be addressed.

(1) Lee, M.; Durst, R. A.; Wong, R. B. *Anal. Chim. Acta* **1997**, *354*, 23–28.

(2) Yap, W. T.; Locascio-Brown, L.; Plant, A. L.; Choquette, S. J.; Horvath, V.; Durst, R. A. *Anal. Chem.* **1991**, *63*, 2007–11.

(3) Patolsky, F.; Lichtenstein, A.; Willner, I. *Angew. Chem., Int. Ed.* **2000**, *39*, 940–943.

(4) Patolsky, F.; Lichtenstein, A.; Willner, I. *J. Am. Chem. Soc.* **2001**, *123*, 5194–5205.

(5) Wang, J.; Cai, X.; Rivas, G.; Shiraiishi, H.; Farias, P. A. M.; Dontha, N. *Anal. Chem.* **1996**, *68*, 2629–2634.

(6) Kaszuba, M.; Jones, M. N. *Biochim. Biophys. Acta* **1999**, *1419*, 221–228.

(7) Baeumner, A. J.; Schmid, R. D. *Biosens. Bioelectron.* **1998**, *13*, 519–29.

(8) Jelinek, R.; Kolusheva, S. *Biotechnol. Adv.* **2001**, *19*, 109–118.

(9) Locascio, L. E.; Hong, J. S.; Gaitan, M. *Electrophoresis* **2002**, *23*, 799–804.

(10) Esch, M. B.; Locascio, L. E.; Tarlov, M. J.; Durst, R. A. *Anal. Chem.* **2001**, *73*, 2952–2958.

(11) Orum, H.; Nielsen, P. E.; Jorgensen, M.; Larsson, C.; Stanley, C.; Koch, T. *BioTechniques* **1995**, *19*, 472–80.

(12) Nielsen, P. E.; Egholm, M.; Berg, R. H.; Buchardt, O. *Science* **1991**, *254*, 1497–500.

(13) Wang, J. *Biosens. Bioelectron.* **1998**, *13*, 757–762.

(14) Bockstahler, L. E.; Li, Z.; Nguyen, N. Y.; Van Houten, K. A.; Brennan, M. J.; Langone, J. J.; Morris, S. L. *BioTechniques* **2002**, *32*, 508–510, 512, 514.

(15) Kim, S. K.; Nielsen, P. E.; Egholm, M.; Buchardt, O.; Berg, R. H.; Norden, B. *J. Am. Chem. Soc.* **1993**, *115*, 6477–6481.

(16) Wittung, P.; Nielsen, P.; Nordén, B. *J. Am. Chem. Soc.* **1996**, *118*, 7049–7054.

(17) Egholm, M.; Buchardt, O.; Christensen, L.; Behrens, C.; Freier, S. M.; Driver, D. A.; Berg, R. H.; Kim, S. K.; Norden, B.; Nielsen, P. E. *Nature* **1993**, *365*, 566–8.

and nonpolar environments is a prime consideration when preparing liposomes hosting PNAs.

Here, we demonstrate a method to incorporate PNAs in phospholipid liposomes where a synthetic di-alkyl "base amphiphile"<sup>19–21</sup> is conjugated to a PNA peptide and natural amino acids (creating a "PNA amphiphile," or PNAA). Co-extrusion eliminates the need for post-extrusion incubation of liposomes and ligands, which can take hours and produce a range of labeling ratios. The covalent linkage allows for the use of PNAA liposomes over a wide range of conditions, including, for example, those that may cause streptavidin–biotin linkages to break.

## Materials and Methods

All solvents (HPLC grade) used in this work were supplied by Fisher Scientific (Pittsburgh, PA). Deionized water was purified in a Barnstead Nanopure Diamond unit to a final resistivity of 18.2 M $\Omega$ -cm. Glassware used for liposome preparation was cleaned using a chromate cleaning solution (Fisher).

**Base Amphiphile Synthesis.** Double-tailed base amphiphiles were synthesized by acid-catalyzed esterification of long-chain alcohols and L-glutamic acid.<sup>20,22</sup> A carboxylic acid headgroup was appended to the lipids by activated coupling of succinic anhydride. The base amphiphile was purified by rotary evaporation and recrystallized three times in ethanol. The purity of both reactions was >98% as measured by electrospray ionization mass spectrometry (Finnigan LCQ).

**PNA Amphiphile (PNAA) Synthesis.** PNAA were synthesized by standard solid-phase peptide synthesis techniques utilizing Fmoc/Bhoc-protected monomers and an Fmoc-protected PAL-PEG-PS resin (0.21 mmol/g loading capacity, Applied Biosystems, Foster City, CA).<sup>23</sup> Fmoc-protected lysine and glutamic acid were acquired from Peptides International (Louisville, KY).

Prior to synthesis, 100 mg of resin was gently shaken in dichloromethane (DCM) for several hours to swell the resin and expose reactive sites. The resin was then deprotected with 20 vol % piperidine in *N,N*-dimethylformamide (DMF) for 8–12 min. Upon deprotection, monomers were added in 5-fold excess (on the basis of the number of resin sites available) to increase product yield. The monomer was activated by mixing equal volumes of monomer, PNA base solution (Applied Biosystems), and PNA activator (Applied Biosystems). The former consists of a mixture of 2,6-lutidine and *N,N*-diisopropylethylamine (DIPEA) in DMF, and the latter is a solution of *O*-(7-azabenzotriazol-1-yl)-1,1,3,3-tetramethyluronium hexafluorophosphate (HATU) in DMF.

After a 2-min activation, the solution was added to the deprotected resin for monomer coupling. For the first coupling, 1-h incubation time was required to maximize the number of coupled sites. Subsequent couplings were performed for 20 min. After coupling, the resin was washed with DMF and DCM, and a small fraction was collected for a ninhydrin test. Unreacted sites were capped by incubation with acetic anhydride (10 min). The resin was again washed with DCM and DMF, and the process was repeated until the desired peptide sequence was complete. The base amphiphile was attached to the N-terminus of the chain, following this procedure, as a final step in the synthesis.

The resin was incubated with 4:1 trifluoroacetic acid (TFA): *m*-cresol for 2 h to cleave the product from the resin and protecting groups. The cleavage cocktail (containing PNAA product) was separated from the resin by filtration and injected directly into a semi-prep HPLC system (Waters Delta 600, Symmetry300 C4

**Table 1. Comparison of PNAA Molecular Weight Values from Mass Spectrometry ( $[M+H]^+_{\text{exp}}$ ) to Values Calculated from Chemical Structures ( $[M+H]^+_{\text{theo}}$ )**

PNAA	$[M+H]^+_{\text{exp}}$ (Da)	$[M+H]^+_{\text{theo}}$ (Da)
(C <sub>14</sub> ) <sub>2</sub> -(AEEA) <sub>2</sub> -agtgatctac-(Glu) <sub>4</sub>	4158.47	4154.97
(C <sub>14</sub> ) <sub>2</sub> -agtgatctac-(Glu) <sub>4</sub>	3867.56	3864.65
(C <sub>14</sub> ) <sub>2</sub> -tttccg-(Lys) <sub>2</sub>	2489.08	2489.77
(C <sub>14</sub> ) <sub>2</sub> -Ser(P)-g	1097.47	1097.40

column, 5- $\mu$ m particle size) for purification. A 40-min linear gradient from 100% water + 0.1% TFA to 100% acetonitrile + 0.1% TFA at 20 mL/min was used. The product peak was lyophilized for storage. Yields for these PNAA syntheses were typically 60% (on the basis of the number of reactive sites on the resin), or 10–15  $\mu$ mol of product per synthesis.

MALDI-TOF mass spectroscopy (PerSeptive Voyager STR) was performed on the product using a matrix of  $\alpha$ -cyano-4-hydroxycinnamic acid. Spectra were acquired with positive polarity (accelerating voltage = 20 kV) in reflector mode. Table 1 lists the  $[M+H]^+$  values for the PNAA discussed here, showing good agreement between the expected and observed molecular weights.

**Naming Convention.** The naming convention used here lists the PNA peptide sequence in the N to C direction from left to right (Figure 1). PNA sequences listed in the N to C direction follow the same Watson–Crick base pairing rules as the corresponding DNA sequence listed in the 5' to 3' direction. The resin used leaves a terminal amine group at the C terminus. PNA nucleobases are in lower case to distinguish them from DNA nucleobases (upper case). The three-letter abbreviation is used for the natural amino acids, and the length of the *n*-alkane chain is the subscript under "C."

**Liposome Extrusion.** Cholesterol (Avanti Lipids) and distearylphosphatidylcholine (DSPC, Avanti Lipids) were dissolved in chloroform to a concentration of 10 mg/mL. PNAA was added to the mixture from a stock solution of known concentration (1 mg/mL in 1:1 chloroform:methanol). The mixture (PNAA: DSPC: chol 5:75:20) was then vortexed and lyophilized. The resulting dry lipid film was hydrated in 50 mM Tris buffer (1.5 mL, pH = 8.0) to a final lipid concentration of 2 mM. The suspension of multilamellar vesicles (MLVs) was subjected to 5–10 freeze–thaw cycles before extrusion through two 0.1- $\mu$ m Nuclepore filters (Whatman, Clifton, NJ) in a stainless steel extruder (Northern Lipids, Vancouver, Canada). Ten extrusion cycles were performed at 60 °C and 350 psi to yield small unilamellar vesicles (SUVs) with a narrow size distribution. This relatively high temperature was necessary to ensure that all lipids were in the fluid phase. Extrusion at room temperature generally resulted in filter blockage.

**Characterization of PNAA Liposomes.** Size distributions for PNAA liposomes were obtained by dynamic light scattering (DLS, Malvern Zetasizer 3000HS). The Zetasizer 3000HS also provided zeta potential distributions using laser Doppler velocimetry. Both measurements were made immediately after extrusion, without further dilution of the extrudate. DLS data were averaged over 10 runs, and the autocorrelation function fitted using the CONTIN method provided by the instrument software.<sup>24</sup> CONTIN is a generic model that allows for fitting of multimodal distributions. CONTIN fitting yielded a single population of PNAA liposomes, with a hydrodynamic diameter comparable to those obtained using single-mode models. Zeta potential data were averaged over five runs, with an applied voltage of 150 V and a current of approximately 8 mA. A second set of DLS measurements were also carried out after zeta potential measurements to ensure that liposomes remained intact in the presence of the electric field.

UV spectra (Varian Cary 300) were collected on the extruded SUVs to assess the total amount of PNAA in the extrudate. UV scans were performed at room temperature with 1-cm quartz cuvettes and a fixed range of wavelengths (500–200 nm). The following extinction coefficients (260 nm) were used for the PNA

(18) Wittung, P.; Kajanus, J.; Edwards, K.; Nielsen, P.; Norden, B.; Malmstroem, B. G. *FEBS Lett.* **1995**, *365*, 27–9.

(19) Gore, T.; Dori, Y.; Talmon, Y.; Tirrell, M.; Bianco-Peled, H. *Langmuir* **2001**, *17*, 5352–5360.

(20) Yu, Y. C.; Pakalns, T.; Dori, Y.; McCarthy, J. B.; Tirrell, M.; Fields, G. B. *Methods Enzymol.* **1997**, *289*, 571–87.

(21) Yu, Y.-C.; Tirrell, M.; Fields, G. B. *J. Am. Chem. Soc.* **1998**, *120*, 9979–9987.

(22) Berndt, P.; Fields, G. B.; Tirrell, M. *J. Am. Chem. Soc.* **1995**, *117*, 9515–22.

(23) Vernille, J. P.; Kovell, L. C.; Schneider, J. W. *Bioconjugate Chem.* **2004**, *15*, 1314–1321.

(24) Provencher, S. W. *Comput. Phys. Commun.* **1982**, *27*, 213–227.

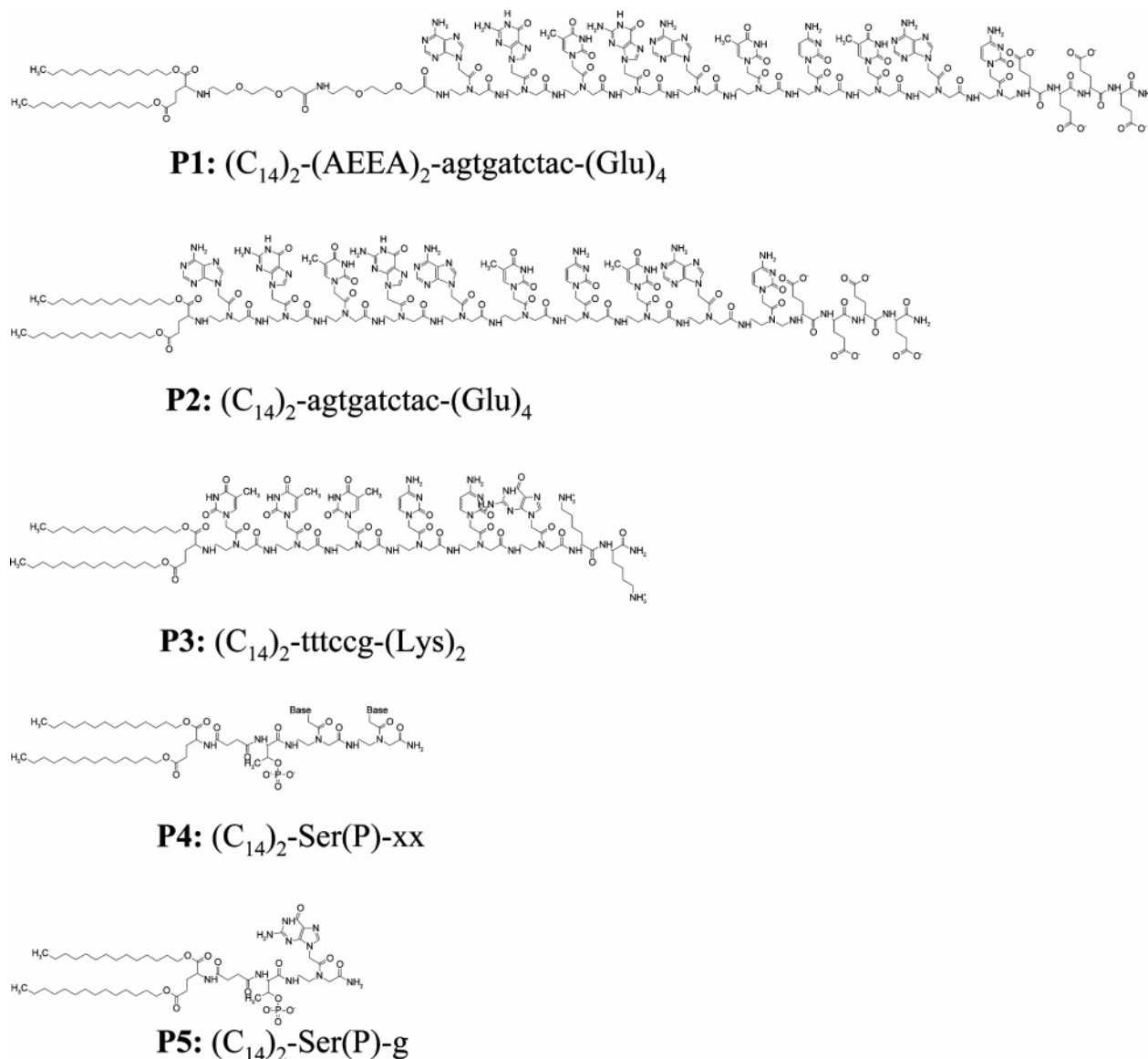


**Figure 1.** Chemical structures of di-alkyl PNA amphiphiles (PNAAs).

monomers (A,G,T,C):  $\epsilon_A = 13\,700\text{ L mol}^{-1}\text{ cm}^{-1}$ ,  $\epsilon_G = 11\,700\text{ L mol}^{-1}\text{ cm}^{-1}$ ,  $\epsilon_T = 8600\text{ L mol}^{-1}\text{ cm}^{-1}$ ,  $\epsilon_C = 6600\text{ L mol}^{-1}\text{ cm}^{-1}$ .<sup>25</sup>

**Capillary Zone Electrophoresis (CZE).** DNA oligomers were obtained from Integrated DNA Technologies (Coralville, IA) and used as received. DNA purity was measured by anion-exchange chromatography with a Waters Spherisorb S5 SAX column (80 Å pore size, 5- $\mu\text{m}$  particle size) and was determined to be >95%. Stock solutions of DNA oligomers were prepared in 50 mM Tris buffer (pH 8.0). The concentration of DNA in the stock solutions was determined by UV measurements, as described above, to be approximately 1 mM.

Detection of DNA binding to PNAAs liposomes was carried out in a Beckman P/ACE MDQ CE system equipped with a UV detector and a liquid-cooled capillary cartridge. Experiments were performed in a fused silica capillary (50  $\mu\text{m}$  i.d., 21.0 cm length to detector, 31.2 cm total length) at 22 °C. Prior to injection, an amount of DNA equimolar to the PNAAs concentration was added to 50  $\mu\text{L}$  of extrudate and was allowed to stand for 4.5 h at 10 °C in the refrigerated compartment of the instrument. Samples were introduced into the capillary by hydrodynamic injection (0.5 psi for 5 s) and eluted under normal polarity with an electric field of 240  $\text{V cm}^{-1}$  using a running buffer of 50 mM Tris (pH 8.0). Elution peaks were detected at 254 nm, and a neutral

marker (50  $\mu\text{M}$  benzyl alcohol) was used in each run to determine the magnitude of electroosmotic flow (EOF) in the uncoated capillary.

The apparent electrophoretic mobility ( $\mu_{\text{app}}$ ) of the liposomes and unbound DNA, as well as the electroosmotic mobility ( $\mu_{\text{EOF}}$ ) in each experiment, were calculated from migration time ( $t$ ) data by the following equations:

$$\mu_{\text{app}} = \frac{l}{tE} = \frac{lL}{tV} \quad (1)$$

$$\mu_{\text{EOF}} = \frac{l}{t_{\text{EOF}}E} = \frac{lL}{t_{\text{EOF}}V} \quad (2)$$

where  $l$  is the effective length of the capillary,  $E$  is the electric field,  $L$  is the total length of the capillary, and  $V$  is the applied voltage. The effective mobility ( $\mu_{\text{eff}}$ ) is then calculated by subtracting  $\mu_{\text{EOF}}$  from  $\mu_{\text{app}}$ :

$$\mu_{\text{eff}} = \mu_{\text{app}} - \mu_{\text{EOF}} \quad (3)$$

All data collection and peak analysis (integration) were done with Beckman P/ACE 32 Karat software. The extent of DNA binding to PNAAs liposomes was estimated from the reduction in the DNA peak area upon addition of liposomes. This value was then normalized by the number of PNA strands on the outer

(25) *Peptide Nucleic Acids: Protocols and Applications*, 2nd ed.; Nielsen, P. E., Ed.; Horizon Bioscience: Norfolk, 2004.

lipid bilayer (0.5) to obtain the percent of available PNAA duplexed with DNA (%dup):

$$\%dup = 2 \left( 1 - \frac{A}{A_0} \right) \frac{[DNA]}{[PNA]} \times 100\% \quad (4)$$

where  $A$  and  $A_0$  correspond to DNA peak areas with and without liposomes, respectively.  $[DNA]$  is the total concentration of DNA strands in the samples, and  $[PNA]$  is the total concentration of PNA strands in the system. The number of PNA strands on the outer layer was taken to be 0.5, but this assumption of equal distribution of PNAA in both inner and outer layers was not tested experimentally.

**Pressure–Area Isotherms.** Pressure–area isotherms were collected using a computer-controlled, water-cooled KSV5000 Langmuir trough operated in a dust-free laminar flow hood. Surface pressure was measured by a platinum Wilhelmy plate. For these measurements, PNAA was dissolved in 1:1 chloroform:methanol to a concentration of 1 mg/mL. Approximately 200  $\mu$ L of this solution (0.05–0.1  $\mu$ mol, depending on the molecular weight of the PNAA) was spread onto the subphase. All isotherms were collected at room temperature in a 50 mM Tris subphase at pH 8.0, maintaining a constant rate of surface pressure increase throughout the isotherm.

**Quartz Crystal Microgravimetry (QCM).** Microgravimetric measurements were performed in a Q-sense D300 QCM with a silica-coated quartz crystal. The QCM was cleaned with 2 vol % Hellmanex (Hellma GmbH, Mullheim, Germany) for 1 h and then flushed with water. Before being mounted in the QCM, the crystal was soaked in 2 vol % sodium dodecyl sulfate (SDS) overnight, rinsed copiously with water, dried under a nitrogen stream, and cleaned in a UV chamber for 30 min. After the QCM was properly assembled with the crystal, 50 mM Tris buffer (pH 8.0) was added, and the normalized frequency monitored. Once a steady baseline was established, 0.5 mL of sample ([lipid] = 0.18 mM) was introduced into the chamber and the normalized frequency was recorded.

## Results and Discussion

### Design of Bioactive, Processable Di-Alkyl PNAA.

Because PNAs are more nonpolar than natural peptides and are poorly soluble in water, an initial challenge was to design a PNAA that possessed sufficient hydrophilic/lipophilic balance so that the headgroups could be hydrated under normal processing conditions while forming stable liposomes that present PNAA in a bioactive form. We have developed a series of water-soluble, micelle-forming PNAA with single  $n$ -alkane chains,<sup>23</sup> and an early attempt was to form SUVs of phospholipids and allow mono-alkyl PNAAs to adsorb to the surface.<sup>26</sup> Since no significant adsorption of mono-alkyl PNAAs to phospholipid SUVs was observed, we turned to co-extrusion of di-alkyl PNAAs with phospholipids. The low extent of PNAA adsorption to vesicles agrees with the results of Wittung et al. who ascribed low PNAA efflux rates from phospholipid liposomes to a low solubility of PNAAs in the lipid bilayer.<sup>18</sup>

Several different di-alkyl PNAAs were synthesized and analyzed for their ability to incorporate into extruded SUVs. Poorly hydrated PNAA liposome suspensions had a clumpy appearance and tended to clog the extrusion filter, leading to the development of high pressures. We regarded either of these observations as indicators of poor hydration. PNAAs with the structures  $(C_{16})_2$ -tttccg-Lys,  $(C_{16})_2$ -tctg,  $(C_{16})_2$ -tttccg,  $(C_{14})_2$ -tttccg,  $(C_{14})_2$ -ccc-Lys,  $(C_{14})_2$ -cc-Lys,  $(C_{14})_2$ -c,  $(C_{14})_2$ -a, and  $(C_{14})_2$ -Glu-c were poorly hydrated (see Materials and Methods for nomenclature). PNAA in Figure 1 exhibited good hydration properties and were studied in more detail.

(26) Peitzsch, R. M.; McLaughlin, S. *Biochemistry* **1993**, *32*, 10436–43.

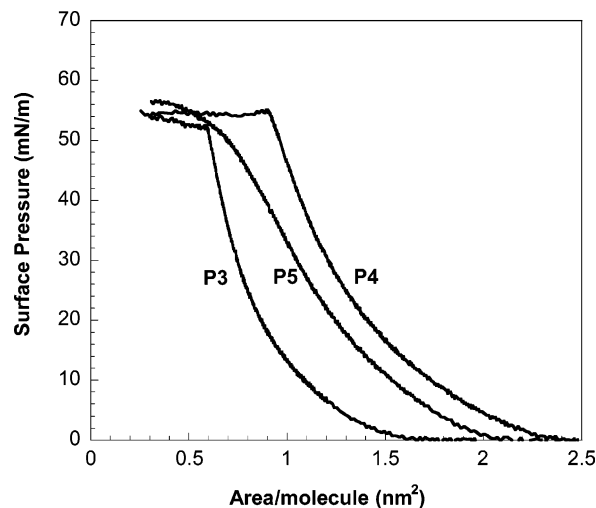


**Figure 2.** Pressure–area isotherms of PNAA with short headgroups at room temperature. P3:  $(C_{14})_2$ -tttccg-(Lys)<sub>2</sub>. P4:  $(C_{14})_2$ -Ser(P)-xx. P5:  $(C_{14})_2$ -Ser(P)-g.

PNAA liposomes prepared from P1–P5 all gave highly monodisperse size distributions, as determined by dynamic light scattering (DLS). After addition of DNA oligomers, liposomes containing P3 reorganized, yielding cloudy suspensions and unphysical results from DLS. In general, we observed such reorganization of PNAA liposomes whenever positively charged lysine residues were added to confer headgroup hydration, but this effect was not tested exhaustively. This electrostatically driven reorganization is a well-known effect observed in cationic liposomes in the presence of plasmid DNA.<sup>27–30</sup> No significant DNA-induced reorganization was observed when phosphoserine (Ser (P)) was used in place of lysine (P4 and P5).

For DNA hybridization studies, we synthesized a molecule containing a lipid double tail, 10 PNA bases, and 4 glutamic acid residues (P2). We were able to properly hydrate this molecule and achieve 85% incorporation in the lipid bilayer (loss of PNAA most likely occurs in the extrusion step because of incomplete hydration of amphiphilic headgroups). We observed a negligible amount of DNA binding to PNAA liposomes of P2, which could be due to steric interference between the phospholipid headgroup (~0.8 nm in length) and one or two PNA bases closest to the surface (~0.7 nm/base).<sup>31,32</sup> While the PNA peptide is much longer than the phospholipid headgroups, it may adsorb flatly onto the liposome surface and become inaccessible for binding from solution. DNA binding results were greatly improved using an ethylene-glycol spacer (8-amino-3,6-dioxaoctanoic acid, AEEA), as discussed below. The use of alkyl spacers led to poor hydration and filter clogging.

**Pressure–Area Isotherms of PNAA.** Figures 2 and 3 show pressure–area isotherms for Langmuir monolayers of P1–P5. The high collapse pressures ( $\Pi_c \sim 55$  mN/m) observed in these isotherms indicate that the monolayers

(27) Raedler, J. O.; Koltover, I.; Salditt, T.; Safinya, C. R. *Science* **1997**, *275*, 810–814.

(28) Koltover, I.; Salditt, T.; Radler, J. O.; Safinya, C. R. *Science* **1998**, *281*, 78–81.

(29) Raedler, J. O.; Koltover, I.; Jamieson, A.; Salditt, T.; Safinya, C. R. *Langmuir* **1998**, *14*, 4272–4283.

(30) Koltover, I.; Salditt, T.; Safinya, C. R. *Biophys. J.* **1999**, *77*, 915–24.

(31) Nagle, J. F.; Tristram-Nagle, S. *Biochim. Biophys. Acta* **2000**, *1469*, 159–195.

(32) Nagle, J. F.; Tristram-Nagle, S. *Curr. Opin. Struct. Biol.* **2000**, *10*, 474–480.

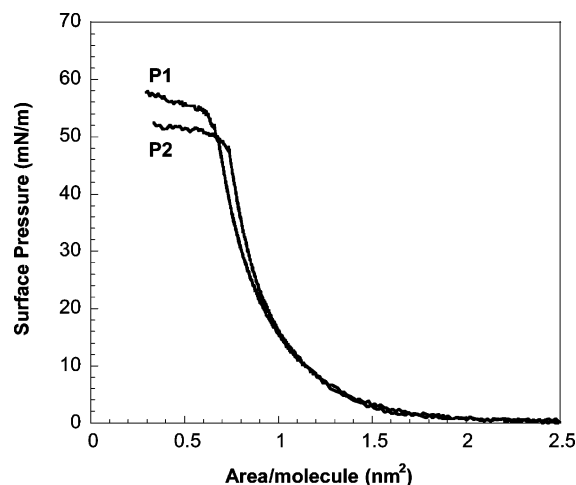


**Figure 3.** Pressure–area isotherms of 10bp PNAA at room temperature. P1:  $(C_{14})_2$ -(AEEA) $_2$ -agtgatctac-(Glu) $_4$ . P2:  $(C_{14})_2$ -agtgatctac-(Glu) $_4$ .

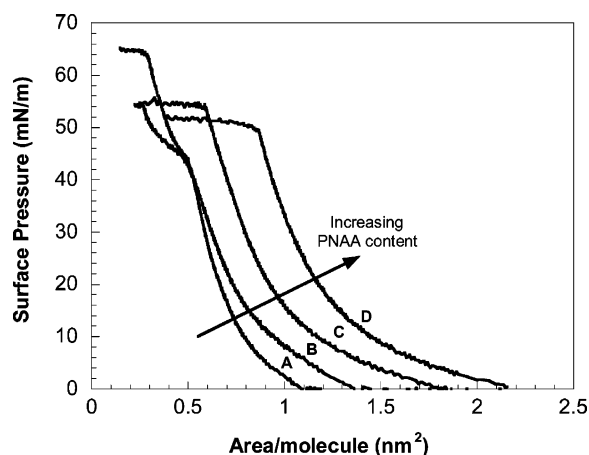


**Figure 4.** Pressure–area isotherms of 10bp PNAA (P1) mixed with DSPC at room temperature. All samples contained 20 mol % cholesterol. A: DSPC:chol 80:20. B: P1: DSPC:chol 5:75:20. C: P1: DSPC:chol 25:55:20. D: P1: DSPC:chol 50:30:20.

are stable and that PNAA are insoluble in the aqueous subphase. All the isotherms have the gradual increase in surface pressure consistent with a liquid-expanded monolayer phase. The isotherms show no pronounced kink corresponding to the peptide headgroup being compressed out of the bilayer, as observed for peptide amphiphiles of collagen peptides.<sup>22</sup> This supports our contention that the PNA peptide headgroup does not interact with the non-polar interior of phospholipid bilayers. Interestingly, the addition of two AEEA spacers yields only a slight increase in collapse pressure and no other significant changes (Figure 3).

To assess the miscibility of P1 with DSPC:cholesterol in liposomes, we collected surface pressure ( $\Pi$ ) versus area isotherms on monolayers with compositions identical to those used in liposome formulation but with varying PNAA mole fraction. Figure 4 shows that a fluid pressure–area isotherm is observed over a large range of PNAA mole fraction (0–50 mol %). The surface phase rule predicts that monolayer components are immiscible if the monolayer collapse pressure is independent of the monolayer composition.<sup>33</sup> Figure 4 shows a large variation in the collapse pressure between the 0 mol % ( $\Pi_c = 63$  mN/m) and 5 mol % ( $\Pi_c = 54$  mN/m) isotherms and smaller but

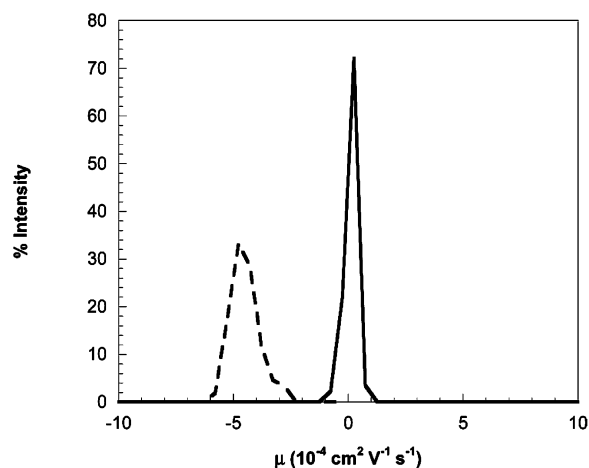


**Figure 5.** Mobility distributions of PNA liposomes (P1: DSPC: cholesterol 5:75:20, dashed curve) and control liposomes (DSPC: cholesterol 80:20, solid curve) measured with the Malvern Zetasizer 3000HS.

significant variations at higher PNAA mol %. This indicates that the three components are miscible in these monolayers, and by extension, in the extruded SUVs. Langmuir–Blodgett deposition of the monolayers gave unacceptably high-transfer ratios over a range of deposition conditions, so imaging of the monolayers using atomic force microscopy or ex-situ epifluorescence microscopy was not possible. A weak transition is observed at  $\Pi = 45$  mN/m for the 0 mol % and 5 mol % cases only and is likely an LE-LC transition for the DSPC:cholesterol monolayer suppressed by the addition of PNAA.

**Characterization of PNAA Liposomes.** Extruded PNAA liposomes with a 5:75:20 composition of P1: DSPC: cholesterol were sized using dynamic light scattering ( $D = 98$  nm) and their electrophoretic mobility ( $\mu = -4.8 \times 10^{-4}$  cm $^2$  V $^{-1}$  s $^{-1}$ ) was measured by laser Doppler velocimetry (LDV). Both measurements were made using the Malvern Zetasizer 3000HS. As shown in Figure 5, the mobility was significantly more negative than that measured for phosphocholine liposomes ( $\mu = 1.3 \times 10^{-5}$  cm $^2$  V $^{-1}$  s $^{-1}$ ), indicating that the negatively charged P1 amphiphile was successfully incorporated into the liposome. In addition, analysis of a PNAA liposome sample using size exclusion chromatography (UV detection) yielded only one peak eluting much earlier than a mono-alkyl PNAA control (no liposomes, data not shown).

To quantify the incorporation of PNAA into SUVs, UV spectra (Figure 6) were collected on the extrudate. To account for Rayleigh scattering and turbidity in the sample,<sup>34,35</sup> we fit power-law curves through the non-absorbing portion of the spectrum (300–500 nm) and obtained the expected power-law exponent of  $-4$ . After subtracting the Rayleigh contribution, the remaining  $A_{260}$  value was used to determine the PNAA concentration in the extrudate, which accounted for PNAA on both the inner and outer portions of the lipid bilayer. From this analysis, nearly all of the PNAA in the initial, unextruded suspension remained in the extruded SUVs, with little detectable adsorption onto the filter during extrusion. The extruded PNAA liposomes were stable for several weeks when stored at 4 °C.

**Hybridization of DNA Oligomers to PNA Liposomes.** DNA binding to PNAA liposomes was assessed

(34) Berti, D.; Barbaro, P.; Bucci, I.; Baglioni, P. *J. Phys. Chem. B* **1999**, *103*, 4916–4922.

(35) Berti, D.; Luisi, P. L.; Baglioni, P. *Colloids Surf., A* **2000**, *167*, 95–103.

(33) Gaines, G. L. *Insoluble Monolayers at Liquid–Gas Interfaces*; Wiley-Interscience: New York, 1966.

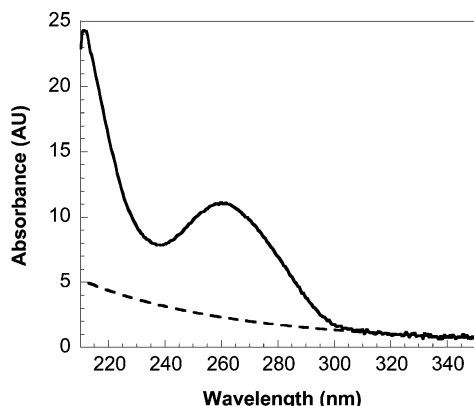


**Figure 6.** UV spectrum (solid curve) of 100 nm PNA liposomes (P1:DSPC:chol 5:75:20). To calculate the amount of PNA in the lipid bilayer, Rayleigh scattering of liposomes was subtracted by fitting a power-law curve (dashed curve) to the nonabsorbing portion of the spectrum (300–500 nm).

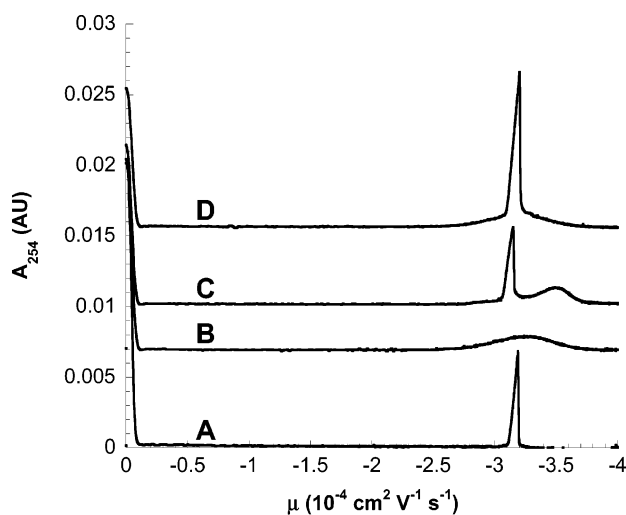


**Figure 7.** Capillary electropherograms showing sequence-specific binding of DNA to PNA liposomes. A: 10bp DNA ( $[DNA] = 85 \mu M$ ). B: PNA liposomes ( $[PNA] = 85 \mu M$ , P1: DSPC:chol 5:75:20). C: PNA liposomes + complementary DNA (5'-GTAGATCACT-3'). D: PNA liposomes + noncomplementary DNA (5'-GTAGAGCACT-3').

using capillary zone electrophoresis (CZE). Prior to injection, a 50- $\mu L$  solution of 100  $\mu M$  PNA (attached to liposomes) and 100  $\mu M$  of a complementary DNA oligomer (5'-GTAGATCACT-3') was prepared in 50 mM Tris buffer (pH 8.0) and placed in a refrigerated compartment of the CZE instrument (10 °C). After a 4.5-h incubation, the sample was injected into an uncoated silica capillary and eluted with a 50 mM Tris running buffer. The resulting CZE electropherogram is shown in Figure 7C (the elution time has been rescaled as electrophoretic mobility, see Materials and Methods). Two peaks are evident: a sharp peak followed by a broad peak. By comparison with electropherograms for pure DNA oligomer (7A), and pure PNA liposome (7B), we conclude that the broad peak of 7C represents PNA liposomes with attached DNA. Because 7A–7C were run with the same concentration of DNA and PNA liposomes, the reduction of the peak area for the DNA oligomer can be used to determine the amount of PNA on the liposome that is duplexed with its DNA complement (%dup), assuming no nonspecific binding and a 50% availability of the PNA (half of the total amount on the outer monolayer). Under these conditions, about 83% of the available PNA was duplexed with DNA from solution. We recognize that the composition of the inner

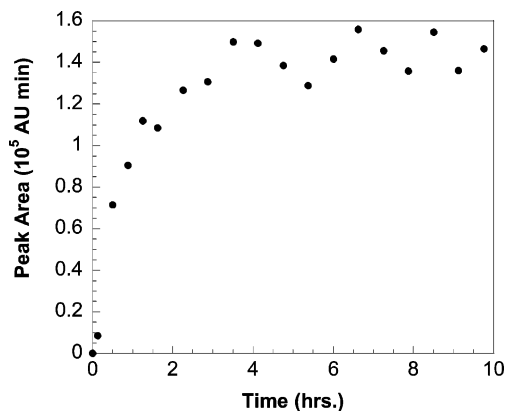


**Figure 8.** Area under PNA liposome–DNA peaks (from CZE) plotted as a function of incubation time. Complete hybridization occurs after 3 h when samples are incubated at 10 °C.

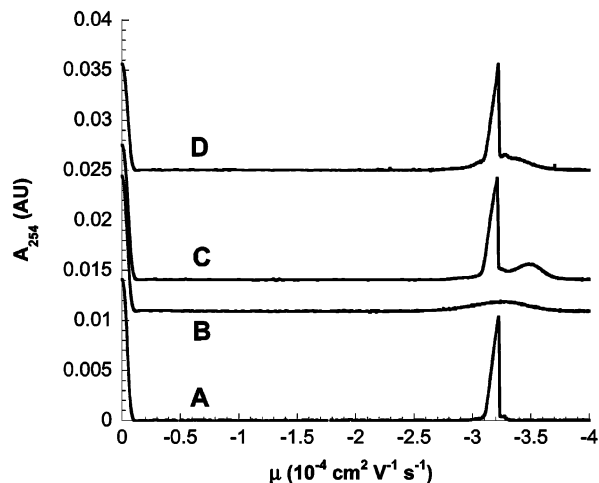
and outer monolayer can vary substantially for SUVs,<sup>36</sup> and this calculation should be regarded as an approximation.

Figure 7D shows results of an identical experiment where the DNA complement has been replaced by a single-mismatch oligomer (5'-GTAGAGCACT-3'). Here, a superposition of 7A (DNA oligomer) and 7B (PNA liposome) is observed, indicating that no surface binding is occurring. Because the two peaks (Figure 7D) coelute, we could not quantify the exact amount of bound DNA in this case, but it appears that the excellent sequence selectivity of PNAs is preserved when attached to liposomes as di-alkyl PNA.

Using the same solution conditions (complementary DNA), we carried out a time-course study of the increase in the area under the putative DNA–PNA liposome peak (“bound area”) and found that it levels off after approximately 3 h at 10 °C (Figure 8). While the time required to achieve binding is much longer than for individual, mono-alkyl PNA in solution,<sup>23</sup> for sensing applications a full recovery of DNA in solution may not be necessary, and a significant amount of DNA binding occurs even after 30 min. The slower kinetics is likely due to the electrostatic barrier presented by the requisite (Glu)<sub>4</sub> groups of P1. Instrumental limitations prevented us from dramatically increasing the ionic strength, or reducing the amount of PNA in each liposome, to test this hypothesis. We further add that since binding was allowed to occur in a 1:1 stoichiometry between the total amount of PNA and DNA, there is likely an effective 2-fold excess of DNA under our assumption that only 50% of the PNA is available for binding.

We also attempted to bind longer DNA targets containing the 10bp target sequence plus four-cytosine overhangs on either end of the binding sequence (Figure 9). While the 3'-overhang DNA (9C) appeared to bind fairly well, the 5'-overhang (9D) DNA did not. This is a bit surprising, since we would expect the 3'-overhang to sterically interfere with the phospholipid headgroups while the 5'-overhang would simply extend into solution. We believe that a compensation of electrostatic repulsion and attractive nonpolar interactions may explain this. Since both DNA oligomers add four negative charges, the electrostatic repulsion engendered by the liposome double layer operates in both cases. However, the 3' overhangs can balance this repulsion by nonspecific, attractive interactions between the nucleobases and the lipid bilayer, regaining the free energy required for hybridization. Another

(36) Yeagle, P. L.; Hutton, W. C.; Martin, R. B.; Sears, B.; Huang, C. H. *J. Biol. Chem.* **1976**, *251*, 2110.



**Figure 9.** Capillary electropherograms showing the binding of longer DNA sequences to PNA liposomes. A: 14bp DNA of a random sequence ([DNA] = 85  $\mu$ M). B: PNA liposomes ([PNAA] = 85  $\mu$ M, P1:DSPC:chol 5:75:20). C: PNA liposomes + 3'-overhang DNA (5'-GTAGATCACTCCCC-3'). D: PNA liposomes + 5'-overhang DNA (5'-CCCGTAGATCACT-3').

possibility is that the 5' overhangs are in closer proximity to the (Glu)<sub>4</sub> residues of P1 and, therefore, pay a larger electrostatic penalty.

Support for the former hypothesis is provided by a control experiment performed on DSPC:cholesterol liposomes with no PNAA. Under the same conditions as above, we observe that approximately 18% of the available DNA (5'-GTAGATCACT-3') strands bind to these non-functional liposomes. Recalling that no significant binding of mismatched DNA could be observed for 5 mol % PNAA, we conclude that (a) the PNAA provides a background repulsion that prevents nonspecific DNA adsorption and (b) attractive, nonspecific interactions do exist between DNA oligomers and the DSPC:cholesterol matrix. These attractive interactions could stabilize hybridization of DNA with 3' overhangs. We carried out similar control experiments with liposomes containing unsaturated (DOPC) and PEGylated (DOPE-PEG2000) phospholipids and observed a high amount of nonspecific DNA adsorption. To reduce the porosity of the lipid bilayer,<sup>37</sup> we switched to a mixture of saturated phospholipids (DSPC) and cholesterol for this work.

An ongoing concern when performing CZE using uncoated capillaries is adsorption to the capillary wall.<sup>38</sup> The reasonable agreement of the CZE-obtained mobility of PNAA liposomes ( $\mu = -4.8 \times 10^{-4} \text{ cm}^2 \text{ V}^{-1} \text{ s}^{-1}$ ) with that obtained from LDV ( $\mu = -3.2 \times 10^{-4} \text{ cm}^2 \text{ V}^{-1} \text{ s}^{-1}$ ) suggests that adsorption is minimal or nonexistent. A more stringent test was provided by quartz crystal microbalance (QCM) studies (Figure 10) of liposome adsorption onto silica substrates. While a sizable drop in normalized frequency occurs when DSPC:cholesterol liposomes are added (demonstrating surface adsorption<sup>39</sup>), no change is observed with 5 mol % PNAA in the liposomal matrix. The presence of the PNAA not only acts to prevent

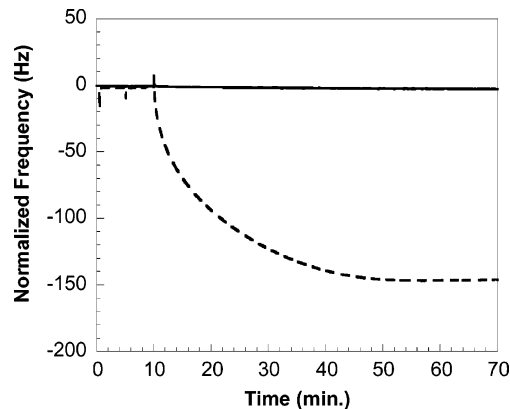


**Figure 10.** Quartz crystal microbalance traces showing the affinity of different liposome formulations to silica surfaces. Samples were injected at  $t = 10$  min. Solid curve corresponds to PNAA liposomes (P1:DSPC:chol 5:75:20), and the dashed curve corresponds to nonfunctionalized liposomes (DSPC:chol 80:20).

nonspecific adsorption of DNA, it also prevents adsorption of the PNAA onto the capillary wall, presumably by electrostatic stabilization.

Efficient binding of blunt DNA (no overhangs) using PNAA liposomes in CZE is demonstrated. While the binding is less efficient for longer DNA oligomers, the PNAA liposomes as they stand should be very useful as highly sequence-specific labels for single-molecule diffusion studies germane to membrane biophysics and biotechnology.<sup>40</sup> Furthermore, we believe increasing the binding repertoire will be straightforward in quiescent systems or those utilizing pressure-driven flow, where electrostatic repulsion can be screened by increased ionic strength without complications arising from electroosmotic flow in CZE.

## Conclusions

We have synthesized peptide nucleic acid amphiphiles composed of PNA sequences ranging from 1 to 10 bases coupled to a di-alkyl lipid tail. By adding appropriate charged amino acid residues and spacers, we have achieved sufficient headgroup hydration and PNA presentation to incorporate these amphiphiles into stable liposomal structures that bind equal-length DNA in a sequence-specific manner. We also found that these PNA liposomes appear to bind DNA with overhanging bases on the 3'-end by a compensation of nonspecific attraction between nucleobases and the lipid bilayer and electrostatic repulsion.

**Acknowledgment.** The authors would like to acknowledge the National Science Foundation (BES-0093538), the Arnold and Mabel Beckman Foundation, and a joint grant from the Air Force Office of Scientific Research and the DARPA SIMBIOSYS program for financial support of this work. We would also like to thank Malvern Instruments (Ana Morfesis) for use of the Zetasizer 3000HS and Jessica Tucker for technical assistance with QCM measurements.

LA047962U

(37) Radko, S. P.; Stastna, M.; Chrambach, A. *Anal. Chem.* **2000**, *72*, 5955–5960.

(38) Reboiras, M. D.; Kaszuba, M.; Connah, M. T.; Jones, M. N. *Langmuir* **2001**, *17*, 5314–5318.

(39) Keller, C. A.; Kasemo, B. *Biophys. J.* **1998**, *75*, 1397–1402.

(40) Yoshina-Ishii, C.; Boxer, S. G. *J. Am. Chem. Soc.* **2003**, *125*, 3696–3697.